Loading Pattern Optimization for OPR-1000 Using Simulated Annealing with Pin-wise Vision Transformer Based Screening Technique

Seongjin Jeong, Hyun Chul Lee*

School of Mechanical Engineering, Pusan National University, 2, Busandaehak-ro 63beon-gil, Geumjeong-gu, Busan, 46241, Korea

*Corresponding author: hyunchul.lee@pusan.ac.kr

INTRODUCTION

To enhance the safety and efficiency of a reactor core, it is crucial to optimize the fuel assembly loading pattern (LP). However, given the vast number of potential LPs, evaluating every possible LP is impractical. Although methods such as simulated annealing (SA) can be employed to search for an optimal solution, they still necessitate a substantial number of LP evaluations. To address this challenge, a screening technique utilizing a simplified model [1] has been proposed. This method can evaluate LPs at a much faster rate compared to traditional 3D deterministic calculations, thus enabling more rapid LP optimization.

Previous research has explored the use of Convolutional Neural Networks (CNNs) for LP evaluation [2]. However, CNNs are designed to analyze images using convolutional filters of fixed sizes, making them more suited for extracting features from relatively small regions. This characteristic of CNN limits their efficiency when dealing with large LP images where each pin is represented as a pixel.

In this study, we aim to enhance the accuracy of LP evaluations by utilizing the Vision Transformer (ViT) model [3]. ViT divides the entire image into small patches and captures the relationships between all patches using a self-attention mechanism. This process helps in extracting features over a broader range compared to the filter-based approach of CNNs. By integrating ViT, we have improved the efficiency of the screening technique, thereby enabling faster execution of SA to identify the optimal LP.

METHODS AND RESULTS

The LPs for the training dataset were generated by shuffling fuel assemblies (FAs) based on the reference LP. First, the FAs located at the center of the core (region 0) do not participate in the exchange. Next, FAs in region 1 and FAs in region 2 are swapped separately. If the exchange of FAs in Region II disrupts the 8th symmetry of the FA types, the symmetry is maintained by swapping the corresponding FAs in the 8th symmetric region. Finally, two FAs of identical type in region 1 are selected and exchanged with two FAs in region 2.

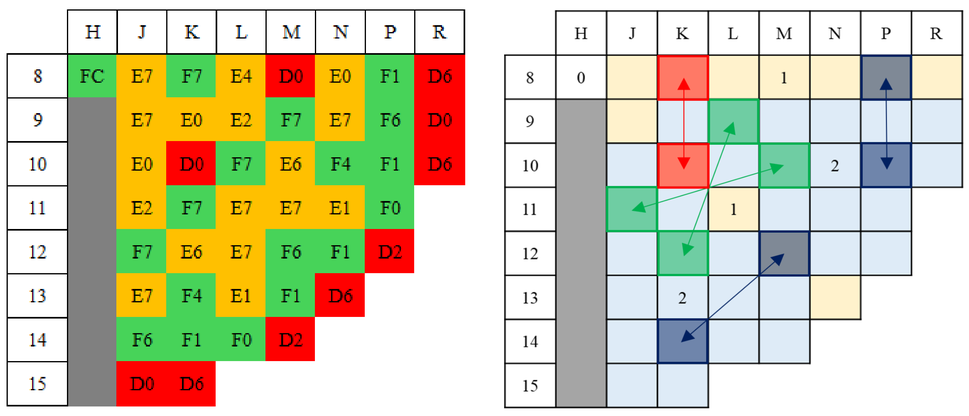

Fig. 1. The reference LP of OPR-1000 [2] and assembly shuffling method. In the reference LP, green indicates fresh fuel, yellow indicates once-burnt, and red indicates twice burnt fuel assembly.

A total of 100,000 LPs were generated. For each LP, the cycle length and peaking factor were calculated using RAST-K code. The cycle length is defined as the Effective Full Power Day (EFPD) at which the critical boron concentration reaches 10 ppm, and the peaking factor represents the maximum value of Fxy in the cycle.

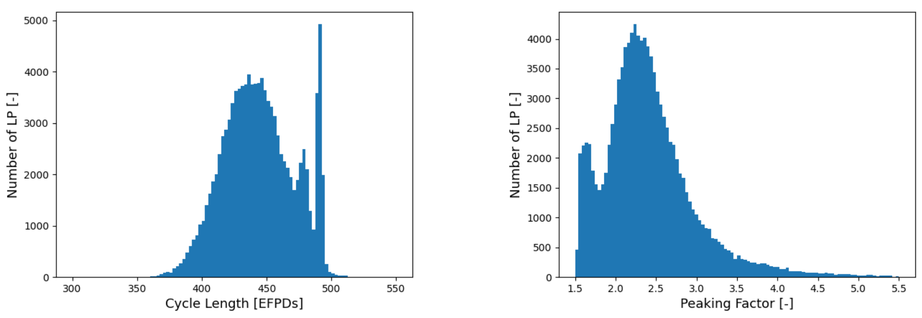

Fig 2. Distribution of cycle length and max-Fxy in the generated LPs.

In the CNN, assembly-wise data is used, which includes the average fuel enrichment, the number of BP rods, the mass fraction of burnable poison, and the initial average burnup for each assembly. In contrast, the ViT uses pin-wise data, which includes the fuel enrichment, mass fraction of burnable absorber, and the 4-unit assembly burnup for each pin. Based on these features, Two models were trained with each architecture, the cycle length prediction model and peaking factor prediction model. When training the models, the entire dataset was split into three portions: 80% was used for model training, 10% for validation during tra[illegible]% f[illegible] was completed.

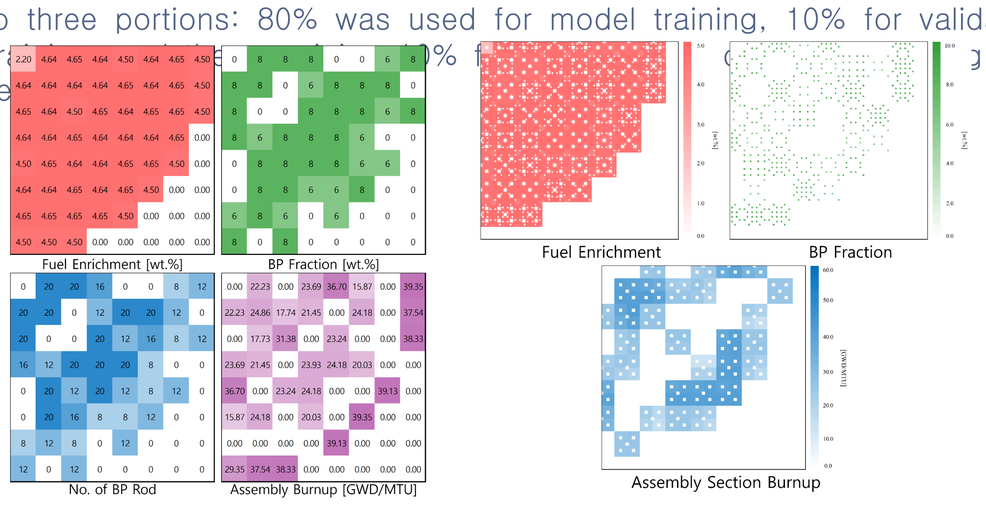

Fig 3. Features of CNN (Left) and ViT (Right) models.

The cycle length prediction model of CNN consists of 9 convolutional layers with a total of 650K parameters. The peaking factor prediction model of CNN, on the other hand, comprises 13 convolutional layers with a total of 1500K parameters. The cycle length prediction model of ViT consists of 3 Transformer encoder layers with a total of 350K parameters. The peaking factor prediction model consists of 9 Transformer encoder layers, with a total of 2,100K parameters.

Comparing the RAST-K calculated values with the AI predicted values. The two graphs for cycle length looks similar, but for the peaking factor, the predictions from the ViT model are more closely clustered around the actual values.

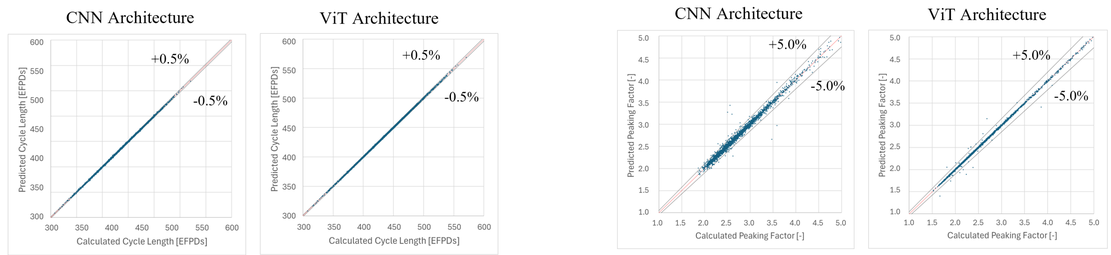

Fig 4. Comparison of RAST-K calculated values with the AI predicted values. Left is for cycle length and right is for max-Fxy.

By utilizing the AI models trained on CNN and ViT architectures, the technique rapidly evaluates candidate LPs, significantly reducing the computational cost compared to full 3D deterministic calculations. However, since AI predictions inherently have some error compared to actual values, this must be considered. For the LPs used in training, the average error ($\overline{\Delta J}$) and standard deviation (σ) of the objective function are calculated by comparing the AI-predicted values with the RAST-K calculated values. These values are then used to define the range within which the true objective value of the current LP may exist. The upper ($J^{3D}_{max}(X)$) and lower ($J^{3D}_{min}(X)$) bounds of this range. If the upper bound of the current LP is lower than the acceptable value, the LP is accepted. Conversely, if the lower bound is higher than the acceptable value, the LP is rejected. If the acceptable value lies within these bounds, a 3D calculation is performed.

$$J^{3D}_{max}(X) = J^{AI}(X) + \overline{\Delta J} + 2\sigma\,,\; J^{3D}_{min}(X) = J^{AI}(X) + \overline{\Delta J} - 2\sigma \qquad \text{(Eq. 1)}$$

If the upper bound of the current LP is lower than the acceptable value, the LP is accepted. Conversely, if the lower bound is higher than the acceptable value, the LP is rejected. If the acceptable value lies within these bounds, a 3D calculation is performed.

In the average results of 20 runs each for CNN-based SA and ViT-based SA. In the case of SA using CNN, the average efficiency was 99.6%, while the efficiency slightly increased to 99.8% when using the ViT. This improvement in efficiency can be attributed to the more accurate peaking factor prediction model used in the ViT-based approach. In the average optimal LP in the SA results. the cycle length and peaking factor of the optimal LP showed almost no difference between the two approaches. This is likely because the AI models have trained with a little of LPs near of the optimal points, which causes the accuracy of the model prediction lower.

Table I: Average of SA results.

AI model	No. of LP evaluations			Efficiency [%]
	RAST-K	AI	Total	
CNN	148	38962	39110	99.6
ViT	99	50570	50669	99.8

Table II: Average optimal LP in the SA results.

AI Model	Cycle Length [EFPDs]	Peaking Factor [-]
CNN	495.5	1.590
ViT	496.1	1.592

CONCLUSION

In this study, we aimThis study developed an ViT-assisted screening technique to enhance the efficiency of SA for optimizing the LP of the OPR-1000 reactor. Comparing CNN-based and ViT-based approaches, the ViT model showed a slight improvement in efficiency (99.8% vs. 99.6%) due to more accurate predictions, especially for the peaking factor. Both approaches yielded similar optimal LPs, indicating that the AI model need more data nearing the optimal LP.

In future research, we plan to incorporate the optimal LP obtained through SA into the AI training dataset, aiming to develop models capable of performing more accurate evaluations in the vicinity of the optimal LP region. By adding more data near the optimal region compared to the existing dataset, the AI will be able to focus on additional learning in that area, leading to more precise LP evaluations. This approach is also expected to enhance the efficiency of the screening technique in the SA process, allowing for the discovery of more optimal LPs in a shorter time frame.

REFERENCE

[1] T. K. Park, H. G. Joo, and C. H. Kim, Multiobjective Loading Pattern Optimization by Simulated Annealing Employing Discontinuous Penalty Function and Screening Technique, Nuclear Science and Engineering, Vol.162, p. 134-147, 2009.

[2] H. Jang, H. C. Shin, D. Kim, and H. C. Lee, Application of Convolutional Neural Network to Fuel Loading Pattern Optimization by Simulated Annealing, Transactions of the Korean Nuclear Society Virtual Autumn Meeting, 2020

[3] A. Dosovitskiy, L. Beyer, A. Kolesnikov, Et Al., AN IMAGE IS WORTH 16X16 WORDS: TRANSFORMER FOR IMAGE RECOGNITION AT SCALE, ICLR, 2021.

[4] J. Park, J. Jang, H. Kim, Et Al., RAST-K v2- Three Dimensional Nodal Diffusion Code for Pressurized Water Reactor Core Analysis, Energies, 13: 6324, 2020.